

Luminex
complexity simplified.



Simple, Compact, and Affordable Cell Analysis.
Muse® Cell Analyzer. [Learn More >](#)



Caspase-8 Serves Both Apoptotic and Nonapoptotic Roles

This information is current as of April 15, 2021.

Tae-Bong Kang, Tehila Ben-Moshe, Eugene E. Varfolomeev, Yael Pewzner-Jung, Nir Yogev, Anna Jurewicz, Ari Waisman, Ori Brenner, Rebecca Haffner, Erika Gustafsson, Parameswaran Ramakrishnan, Tsvee Lapidot and David Wallach

J Immunol 2004; 173:2976-2984; ;
doi: 10.4049/jimmunol.173.5.2976
<http://www.jimmunol.org/content/173/5/2976>

References This article **cites 37 articles**, 15 of which you can access for free at:
<http://www.jimmunol.org/content/173/5/2976.full#ref-list-1>

Why *The JI*? Submit online.

- **Rapid Reviews! 30 days*** from submission to initial decision
- **No Triage!** Every submission reviewed by practicing scientists
- **Fast Publication!** 4 weeks from acceptance to publication

**average*

Subscription Information about subscribing to *The Journal of Immunology* is online at:
<http://jimmunol.org/subscription>

Permissions Submit copyright permission requests at:
<http://www.aai.org/About/Publications/JI/copyright.html>

Email Alerts Receive free email-alerts when new articles cite this article. Sign up at:
<http://jimmunol.org/alerts>

The Journal of Immunology is published twice each month by
The American Association of Immunologists, Inc.,
1451 Rockville Pike, Suite 650, Rockville, MD 20852
Copyright © 2004 by The American Association of
Immunologists All rights reserved.
Print ISSN: 0022-1767 Online ISSN: 1550-6606.



Caspase-8 Serves Both Apoptotic and Nonapoptotic Roles¹

Tae-Bong Kang,^{2*} Tehila Ben-Moshe,^{2*} Eugene E. Varfolomeev,^{3*} Yael Pewzner-Jung,^{*} Nir Yogev,^{*} Anna Jurewicz,[§] Ari Waisman,[¶] Ori Brenner,[†] Rebecca Haffner,[†] Erika Gustafsson,^{||} Parameswaran Ramakrishnan,^{*} Tsvee Lapidot,[‡] and David Wallach^{4*}

Knockout of *caspase-8*, a cysteine protease that participates in the signaling for cell death by receptors of the TNF/nerve growth factor family, is lethal to mice in utero. To explore tissue-specific roles of this enzyme, we established its conditional knockout using the *Cre/loxP* recombination system. Consistent with its role in cell death induction, deletion of *caspase-8* in hepatocytes protected them from Fas-induced caspase activation and death. However, application of the conditional knockout approach to investigate the cause of death of *caspase-8* knockout embryos revealed that this enzyme also serves cellular functions that are nonapoptotic. Its deletion in endothelial cells resulted in degeneration of the yolk sac vasculature and embryonal death due to circulatory failure. *Caspase-8* deletion in bone-marrow cells resulted in arrest of hemopoietic progenitor functioning, and in cells of the myelomonocytic lineage, its deletion led to arrest of differentiation into macrophages and to cell death. Thus, besides participating in cell death induction by receptors of the TNF/nerve growth factor family, caspase-8, apparently independently of these receptors, also mediates nonapoptotic and perhaps even antiapoptotic activities. *The Journal of Immunology*, 2004, 173: 2976–2984.

Programmed cell death was initially thought to occur through induction of death-dedicated cellular proteins. However, it is now known to be mediated mainly by proteins that exist in the cell throughout its life (1). Moreover, some of these proteins display, in addition to their death-oriented function, activities that contribute to the functioning of the living cell. Clarification of the dual nature of these proteins is central to our understanding of the mechanisms of programmed cell death and its physiological significance.

The caspase cysteine protease family is known mainly for the participation of some of its members in programmed cell death in eukaryotes (2). However, increasing evidence suggests that the death-inducing caspases, beside their apoptotic role, also have functions that contribute to activities of living cells (see, e.g., Refs. 3–9). Studies of caspase-8 have focused on the ability of this caspase to interact with receptors of the TNF/nerve growth factor (NGF)⁵ family and to signal for their cell death-inducing effect

(10–12). However, deletion of *caspase-8* in mice resulted in death in utero, which was associated with cardiac deformations, neural tube defects, and hemopoietic progenitor deficiency (13, 14). Because no such phenotype results from targeting of any of the known TNF/NGF family members that use caspase-8 in their signaling, these findings suggested that caspase-8 serves other functional roles as well. In this study, we report the establishment of conditional knockout of the *caspase-8* gene using the *Cre/loxP* recombination system, and its use for exploring these other functions.

Materials and Methods

Generation of mice carrying conditional caspase-8 allele (Casp8^{F/+}) and their use for ubiquitous or tissue-specific inducible deletion of the caspase-8 gene

A targeting construct designed to excise exons 1 and 2 of *caspase-8* upon expression of cyclization recombination enzyme (*Cre*) was assembled in the Bluescript vector by inserting a *loxP* site upstream of the first exon of *caspase-8* and introducing a *NEO⁺TK* (thymidine kinase) cassette flanked by two *loxP* sites (derived from the *loxP-neo* vector; Samuel Lunenfeld Research Institute, Toronto, Ontario, Canada) downstream of exon 2 (see Fig. 1A). The construct contains two DNA stretches derived from the 129 mouse genome, one fragment placed 5' of the first *loxP* site and the other 3' of the "floxed" neo cassette.

NotI-linearized DNA was electroporated into R1 embryonic stem (ES) cells (15), and this was followed by selection with G418. Individual clones were screened for homologous recombination by Southern blot analysis of *EcoRV*-digested DNA, using genomic DNA probes from regions upstream of the 5' arm and downstream of the 3' arm of the targeting construct. The ES cell clones with homologous recombination were transfected with a supercoiled *Cre* recombinase-expressing construct (*EF1a-GFPcre/pBS500*), and this was followed by selection with ganciclovir. *Casp8^{F/+}*-positive ES cell clones with correct deletion of the selection cassette were identified by Southern blot analysis. These ES cells were aggregated with MF-1 blastocysts to generate chimeric mice, which were then mated with MF-1 mice to obtain *Casp8^{F/+}* offspring.

Mice in which one of the *caspase-8* alleles was knocked out and the other floxed (*Casp8^{F/-}*), and which also expressed *Cre* in a tissue- or time-specific manner, were obtained by first mating the various *Cre*-expressing strains (*Tie1-Cre* (16), *Mx1-Cre* (17), *LysM-Cre* (18), *Alb-Cre* (19), or *PGK-Cre* (20)) with mice heterozygous for the *caspase-8* knockout allele (*Casp8^{+/-}*) (13). Offspring that expressed both the *Casp8⁻* allele and the *Cre* transgene were then mated with mice homozygous for the floxed allele, obtained by intercrossing the *Casp8^{F/+}* mice. To visualize tissue-selective

Departments of *Biological Chemistry, †Veterinary Resources, and ‡Immunology, The Weizmann Institute of Science, Rehovot, Israel; §Department of Neurology, Medical University of Lodz, Lodz, Poland; ¶Institute for Genetics, University of Cologne, Weyertal, Cologne, Germany; and ||Department of Experimental Pathology, Lund University Hospital, Lund, Sweden

Received for publication March 17, 2004. Accepted for publication June 21, 2004.

The costs of publication of this article were defrayed in part by the payment of page charges. This article must therefore be hereby marked *advertisement* in accordance with 18 U.S.C. Section 1734 solely to indicate this fact.

¹ This work was supported in part by grants from Ares Trading S.A., Switzerland, the European Union (Grant QLGI-1999-00739), the Kekst Family Center for Medical Genetics at The Weizmann Institute of Science, and the Joseph and Bessie Feinberg Foundation.

² T.-B.K. and T.B.-M. contributed equally to this work.

³ Current address: Department of Molecular Oncology, Genentech, Inc., 1 DNA Way, South San Francisco, CA 94080.

⁴ Address correspondence and reprint requests to Dr. David Wallach, Department of Biological Chemistry, The Weizmann Institute of Science, 76100 Rehovot, Israel. E-mail address: d.wallach@weizmann.ac.il

⁵ Abbreviations used in this paper: NGF, nerve growth factor; BM, bone marrow; BMDC, BM-derived dendritic cells; CFU-S, CFU spleen; Cre, cyclization recombination enzyme; EGFP, enhanced GFP; ES, embryonic stem; MGB, minor groove binder; MHC-II, MHC class II; m, murine; pl-pC, poly(I:C); ΔΔCt, comparative threshold cycle method; MORT1/FADD, mediator of receptor-induced toxicity-1/Fas-associated death domain; Mx1, myxovirus resistance-1; CFU-C, CFU culture.

expression of functional Cre, some of the offspring of the latter mating were mated with the *ZEG* reporter mouse strain that expresses enhanced GFP (EGFP) upon Cre-mediated excision (21).

To induce deletion of *caspase-8* in mice expressing Cre under the control of the myxovirus resistance-1 (*Mx1*) promoter, mice were injected i.p. with either recombinant type I mouse IFN (10^6 U/mouse, kindly donated by Dr. C. Weissmann) (Imperial College School of Medicine at St. Mary's, London, U.K.) or poly(I:C) (pI-pC) dsRNA (5) (250 μ g/mouse; Sigma-Aldrich, St. Louis, MO). Unless otherwise indicated, the mice were injected with pI-pC three times at 2-day intervals. Liver cell or bone marrow (BM) cell function of the *Mx1*-Cre-expressing mice was assessed 2 days after injection of IFN or pI-pC.

In all experiments, the phenotype of the Cre-expressing *Casp8*^{F/+} mice was compared with that of Cre-expressing *Casp8*^{F/+} mice from the same litter. In terms of all the parameters tested in this study, the phenotype of the Cre-expressing *Casp8*^{F/+} mice was indistinguishable from that of wild-type mice, irrespective of the Cre strain used.

Genotyping the mice

Genotyping of the various *caspase-8* alleles was done by Southern blot and PCR analyses of tail DNA. Southern blots were analyzed after digestion of the DNA with *EcoRV*, using genomic DNA probes from regions upstream of the first exon and the 5' arm, and downstream of the 3' arm (between exons 5 and 6) of the targeting construct (Fig. 1, A and B). For the PCR analyses, we used the oligonucleotides 5'-TAGCCTCTTTGGGGTTGT TCTACTG-3' (sense) and 5'-TGGGGCTTCGTTTAGTCTCTACTTC-3' (antisense) for the knockout allele, 5'-TAGCCTCTTTGGGGTTGT TACTG-3' (sense) and 5'-CGCGGTCGACTTATCAAGAGGTAGAAGAG CTGTAAC-3' (antisense) for the floxed allele, and 5'-CGTTGATGCCGGTGA ACGTG-3' (sense) and 5'-AGCTGGCTGGTGGCAGATGG-3' (antisense) for the *Cre* transgenes.

Assessing the consequences of Fas triggering in vivo

Mice were injected i.p. with anti-Fas Ab (Jo-2, 15 μ g/mouse; BD Biosciences, San Diego, CA). Tissues were harvested at the indicated times afterward. Caspase expression and processing were analyzed by Western blotting using rat anti-mouse caspase-8 mAb (1G12; kindly donated by Drs. A. Strasser and L. A. O'Reilly, Walter and Eliza Hall Institute, Melbourne, Australia) and anti-mouse caspase-3 (H-227; Santa Cruz Biotechnology, Santa Cruz, CA), after extraction of the tissues in cell-lysis buffer (20 mM Tris-Cl (pH 7.4), 135 mM NaCl, 1 mM EDTA, 1% Triton X-100, and 10% glycerol) containing 1 \times complete protease inhibitor mixture (Roche Diagnostics, Mannheim, Germany).

Histology and immunostaining

Embryos and the tissues of adult mice were fixed in 10% phosphate-buffered formalin pH 7.4, embedded in paraffin, cut into 4- μ m sections, and stained with H&E. To detect cells expressing processed caspase-3, paraffin sections of E10.5 embryos were deparaffinized, rehydrated, and incubated with anticaspase-3 (Asp¹⁷⁵) Ab (no. 9661; Cell Signaling Technology, Beverly, MA), according to the manufacturer's instructions. This was followed by staining either with Cy3-conjugated goat anti-rabbit Ab (Jackson ImmunoResearch Laboratories, West Grove, PA) or (for immunohistochemical detection) with biotinylated peroxidase anti-rabbit secondary Ab (DAKO Envision+ System, peroxidase (3-amino-9-ethyl carazole); DakoCytomation, Glostrup, Denmark). Immunofluorescent sections were observed with a confocal microscope (LSM 510; Carl Zeiss, Thornwood, NY), using an excitation wavelength of 543 nm and differential interference contrast optics. The immunostained cells were quantified using the ImagePro program (Media Cybernetics, Silver Spring, MD), with at least 2500 cells examined in each of 10 yolk sacs of *Casp8*^{F/+}:*Tie1*-*Cre* embryos and 10 yolk sacs of *Casp8*^{F/+}:*Tie1*-*Cre* embryos.

For whole-mount staining with Ab against PECAM-1 (CD31), yolk sacs were dissected in PBS, fixed for 2 h at 4°C in 2% paraformaldehyde, washed overnight at 4°C in PBS, and treated for 1 h at 4°C in PBS containing 0.3% H₂O₂. After three washings with PBS, the embryos and yolk sacs were incubated for 1 h at 4°C in blocking solution (Casblock; Zymed Laboratories, San Francisco, CA) containing 0.1% Triton X-100, and were then incubated overnight at 4°C with rat anti-mouse PECAM-1 Ab (BD Biosciences) in the same blocking solution. The embryos and yolk sacs were then washed five times, each for 1 h at 4°C in PBS, and incubated overnight at 4°C with biotinylated peroxidase donkey anti-rat Ab (Jackson ImmunoResearch Laboratories) in the same blocking solution. After five more washings, each for 1 h at 4°C, staining was completed using the Vectastain ABC kit (Vector Laboratories, Burlingame, CA) according to the manufacturer's instructions. The color was resolved with 3,3'-diaminobenzidine (Sigma-Aldrich).

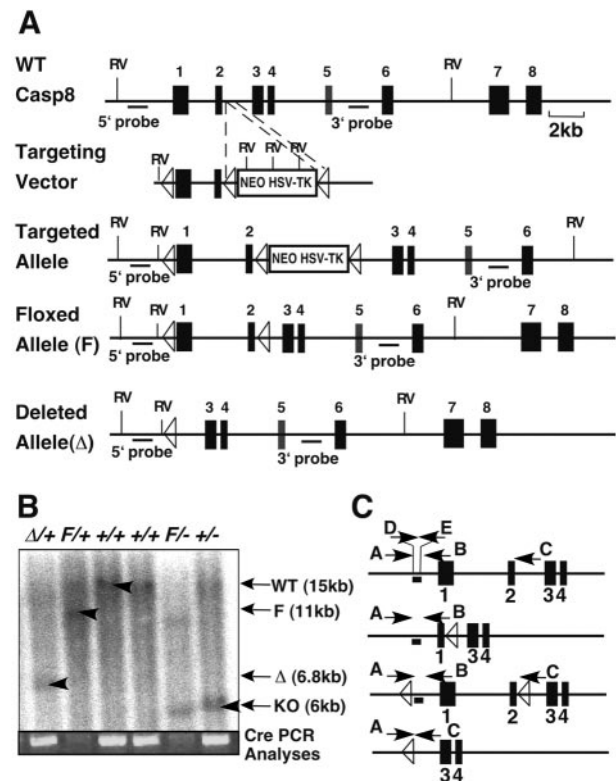


FIGURE 1. Generation of conditional *caspase-8* knockout mice and assessment of Cre-mediated deletion. **A**, Schematic representation of the targeting strategy. The figure shows the structure of the mouse *caspase-8* gene before and after its recombination with the targeting vector and after deletion of the *NEO*⁺*TK* cassette, as well as after further deletion of its floxed region. The positions of the *loxP* sites are designated by triangles. The exons, deduced by comparison with the cDNA sequence, are denoted by black boxes. The positions of the 5' and 3' external genomic DNA probes used for Southern blot analysis of the recombination are underlined. *EcoRV* restriction sites (RV) are marked by vertical lines. **B**, *Cre-loxP*-mediated deletion of the flanked *caspase-8* gene. Southern blot analysis (using the 3' probe shown in **A**) of DNA from the littermate mice obtained by crossing *Casp8*^{F/+} mice with the *Casp8*^{F/+}:*PGK-Cre* transgene. PCR assessment of occurrence of the *Cre* transgene is shown at the bottom. The 6.8-kb fragment corresponding to the deleted floxed allele (Δ) could be observed only in floxed mice that also expressed *Cre*. Homozygous deletion and combination of the deleted and knockout (ko) allele were lethal in utero and could be found only in embryos before midgestation. **C**, Genomic location of the oligonucleotide sequences used to assess the extent of *caspase-8* deletion by PCR (**A**–**C**) and by real-time PCR (**D**–**E**). The figure shows the locations of oligonucleotides used to assess levels of the wild-type (WT), targeted (floxed, F), knockout (KO), and deleted floxed (Δ) *caspase-8* alleles. The underlying short bar corresponds to the genomic region whose level was assessed by real-time PCR.

Flow cytometric analysis

To exclude dead cells, propidium iodide (Sigma-Aldrich) was included in all staining. For quantification of progenitor cell levels in the BM, single-cell BM suspensions were stained with allophycocyanin-anti-CD117 Ab (*c-kit*, 2B8; eBioscience, San Diego, CA) and biotin-conjugated Abs for lineage (Lin) markers (CD3, I45-2C11; B220, RA3-6B2; Mac-1, M1/70; Gr-1, RB6-8C5; TER119) (BD Pharmingen, San Diego, CA) and stained using PE-conjugated streptavidin (BD Pharmingen). Dying cells in the BM culture were quantified by staining of the nonattached cells with PE-anti-CD11b (M1/70) Ab and FITC-Annexin V. (Note that the cells were gated for lack of propidium iodide staining, and thus, their annexin V staining indicates an early stage of death.) Mature macrophages were stained with APC-anti-CD11b (M1/70) Ab and PE-anti-F4/80 Ab (MCA 497PE; Serotec, Oxford, U.K.). T and B cells in lymphoid organs were analyzed after

the cells were stained with PE-anti-B220 (RA3-6B2; eBioscience), allophycocyanin-anti-IgM (II41; BD Pharmingen), PE-anti-CD4 (RM4-5; BD Pharmingen), and allophycocyanin-anti-CD8 (53-6.7; eBioscience) Abs. PE-anti-Ly6G (IA8; BD Pharmingen) and allophycocyanin-anti-CD11b Abs were used for granulocyte analysis, and allophycocyanin-anti-CD11c (N418) and PE-anti-MHC class II (PE-anti-MHC-II) (M5/14.15.2; eBioscience) were used for dendritic cell analysis. Before staining, the cells were incubated with Fc-block (anti-CD16/32 Ab; BD Pharmingen) to block nonspecific Ab binding. Stained cells were analyzed on a FACS-Calibur using the CellQuest software (BD Biosciences).

In vitro progenitor assay

Hemopoietic progenitors in mouse embryos were assayed as previously described (13). To determine the number of clonogenic BM progenitors, single-cell suspensions were harvested from the femoral BM and the nucleated cells were counted and diluted to 2×10^5 cells/ml in IMDM containing 2% FCS. For each myeloid clonogenic progenitor assay, 2×10^4 cells were mixed with 1 ml of methylcellulose medium containing recombinant murine stem cell factor, recombinant murine (m)IL-3, recombinant human IL-6, and erythropoietin (M3434; StemCell Technologies, Vancouver, British Columbia, Canada). The cells were plated and grown in humidified chambers at 37°C and 5% CO₂. After 10–14 days, erythroid burst-forming unit, CFU granulocyte-macrophage, and CFU granulocyte-erythroid-megacaryocyte-macrophage progenitors were scored by microscopic analysis. Colony identification was confirmed by staining of sampled colonies with May-Grünwald-Giemsa stain. CFU B cells were assayed by plating BM suspension (5×10^4 cells) in a methylcellulose medium (M3630; StemCell Technologies) supplemented with 10 ng/ml IL-7, and scoring the colonies after 7 days of incubation. CFU granulocytes were assayed by culturing samples of 1×10^5 BM cells for 7 days in a methylcellulose medium supplemented with 20 ng/ml mrG-CSF (PeproTech, Rocky Hill, NJ) as described (22). Cell patterns in the colonies were assessed by May-Grünwald-Giemsa staining.

In vivo CFU spleen (CFU-S) assays

For the CFU-S assay, BM from pI-pC-treated *Casp8^{F/+}:Mxl-Cre* and *Casp8^{F/-}:Mxl-Cre* mice were depleted of mature T cells using anti-mouse CD4 (L3T4) and CD-8 (Ly-2) MicroBeads (Miltenyi Biotec, Bergisch Gladbach, Germany). Single-cell suspensions (1×10^5 cells) were then injected into the tail veins of irradiated (8.5 Gy, ¹³⁷C source) 10-wk-old C57BL/6 female mice. In each experiment, cells from each donor were injected into ten recipient mice. The recipients were treated with Ciproxin (Bayer, Leverkusen, Germany) in their drinking water (6.7 mg/l) throughout the experiment. Mice were killed 8 or 13 days after transplantation. Spleens were weighed and fixed in Bouin's solution. Colonies were counted under the microscope.

Generation of radiation chimera

BM cells (2×10^6 per recipient) harvested from the femora of *Casp8^{F/+}:Mxl-Cre* and *Casp8^{F/-}:Mxl-Cre* (Ly5.2) mice were injected into irradiated (8.5 Gy, ¹³⁷C source) C57BL/6-Ly5.1 recipient mice (Charles River Laboratories, Lyon, France) via the tail vein or, conversely, BM cells from C57BL/6-Ly5.1 mice were injected into the tail veins of similarly irradiated *Casp8^{F/+}:Mxl-Cre* and *Casp8^{F/-}:Mxl-Cre* recipients. After 8–10 wk, the recipient mice were injected with pI-pC to induce deletion of *caspase-8*, and BM cells derived from these mice were assayed for CFU as described above. Donor engraftment in the recipient mice was quantified by using FITC-CD45.2 (anti-Ly5.2, clone 104) and PE-CD45.1 (anti-Ly5.1, clone A20) Abs, and was found to be over 95%.

Reconstitution of T and B lymphocytes in RAG-1^{-/-} mice

Casp8^{F/+}:Mxl-Cre and *Casp8^{F/-}:Mxl-Cre* mice were injected with pI-pC to induce deletion of *caspase-8*, and their femoral BM cells were harvested and transplanted (1×10^6 cells per recipient mouse) into irradiated (4 Gy, ¹³⁷C source) RAG-1^{-/-} mice (The Jackson Laboratory, Bar Harbor, ME) via the tail vein. The recipient mice were euthanized 7 wk or 6 mo after transplantation, and their BM and lymphoid organ cells were harvested and analyzed.

Preparation of BM-derived and peritoneal macrophages

Primary cultures of BM-derived macrophages were generated from 3- to 4-mo-old mice. Femoral BM cells were cultured with DMEM supplemented with 20% FCS and 30% L929 cell-conditioned medium. After overnight culture, nonadherent cells were harvested and suspended in fresh medium. Aliquots of 2.5×10^5 cells were cultured for 7–10 days at 37°C and 5% CO₂ in 35-mm culture wells. Fresh culture medium was added on day 3 and replaced on day 6. Adherent cells were quantified by the MTT

assay (23) in 96-well plates seeded with 5×10^3 cells per well. More than 90% of the adherent cells stained positively with anti-CD11b and the F4/80 Ab.

Peritoneal cells were harvested by rinsing the mouse peritoneal cavity with sterile PBS (10 ml/mouse) containing 2% FCS. The cells were washed once with PBS and suspended in RPMI 1640 medium supplemented with 10% FCS, glutamine, and penicillin/streptomycin. They were then plated on 35-mm Nunc culture dishes (Nunc, Roskilde, Denmark) at a density of 3×10^6 cells per dish, and cultured for 2–4 h at 37°C and 5% CO₂ to allow macrophage adherence.

Preparation of BM-derived granulocytes and peritoneal neutrophils

Femoral BM cells (see above) were cultured at a density of 5×10^5 cells/ml with RPMI 1640 medium supplemented with 10% FCS and 20 ng/ml mrG-CSF (PeproTech). Granulocyte yield on the 7th day of culturing was assessed by trypan blue exclusion and FACS analysis after immunostaining with anti-Ly6G Ab.

Peritoneal neutrophils were harvested 4 h after injection of 3% thioglycolate (Difco, Detroit, MI) as described (24), followed by purification of Ly6G⁺ cells by MACS magnetic cell separation system (Miltenyi Biotec). FACS analysis using anti-CD11b and Ly6G Abs confirmed that the purity of the cells was >90%.

Preparation of BM-derived dendritic cells (BMDC)

BMDC were prepared as described (25) by culturing femoral BM cells (2×10^5 cells/ml) with RPMI 1640 medium supplemented with 10% FCS, 50 μM 2-ME, and 10 ng/ml mrGM-CSF (PeproTech) for 8 days. Cells were sorted with the aid of anti-CD11c and anti-MHC-II Abs (for isolation of mature MHC-II^{high} and immature MHC-II^{low} BMDC).

PCR and real-time PCR for assessing deletion efficiency

The effectiveness of Cre-mediated deletion of the floxed *caspase-8* allele was roughly estimated by PCR. DNA was extracted from the adherent cultured peritoneal macrophages or BM-derived macrophages, and from liver and spleen samples, as described (26). DNA was subjected to PCR analysis using three primers: 5'-TAGCCTCTTTGGGGTGTCTACTG-3' (A in Fig. 1C; sense for the wild-type, knockout, floxed, and deleted allele), 5'-CCGGTTCGACTTATCAAGAGGTAGAAGAGCTGTAAC-3' (B in Fig. 1C; antisense for the wild-type, knockout, and floxed allele), and 5'-GCGAACACGCCGTGTTTCAAGGGC-3' (C in Fig. 1C; antisense for the deleted allele).

For more precise quantitative evaluation, the extent of deletion was assessed by real-time PCR. The assay was conducted in a reaction volume of 20 μl containing 10 ng DNA, 300 nM oligonucleotide primers, 200 nM oligonucleotide 3'-minor groove binder (MGB) probes, and 10 μl of TaqMan Universal PCR Master Mix (Applied Biosystems, Foster City, CA). Primers and probes were designed using Primer Express software (Applied Biosystems). PCR was initiated by incubating the reaction mixture for 2 min at 50°C for activation of the AmpErase UNG (Applied Biosystems). This was followed by incubation for 10 min at 95°C, and then by 40 cycles of 15 s at 95°C and 1 min at 60°C on an ABI Prism 7000 Sequence Detection System (Applied Biosystems).

Levels of *caspase-8* were normalized on the basis of quantification of the NF-κB-inducing kinase (NIK) gene in the same DNA samples using 5'-AGCCTCTCTACCGCCAGAA-3' (sense), 5'-GTGCCAGACTCTCC TTGCT-3' (antisense), and (5'-6-FAM-ACCAGAACCAGCAAMGB-3' (probe). The comparative threshold cycle method ($\Delta\Delta Ct$) was used to determine the level of *caspase-8* (27). The *caspase-8* oligonucleotide primers applied were 5'-GGAAACAAGCTGGTAGCTGACA-3' (D in Fig. 1C; sense), 5'-CCTGGGTCAACACAAGATGCT-3' (E in Fig. 1C; antisense), and 5'-6-FAM-TTAACCTCCTCACTTGATCAT-MGB-3' (Applied Biosystems). To define the dynamic range and the efficiency of the assay, DNA samples were varied by the use of successive 2-fold dilutions in the range of 0.5–25 ng per reaction. All dilution and negative control samples were tested in triplicate. Analysis of ΔCt at the chosen range of template dilutions confirmed that the plot of log input vs ΔCt has a slope of <0.1, implying that the efficiencies of the real-time PCR for *caspase-8* and for NIK were about equal.

Ct were determined by plotting normalized fluorescent signal against cycle number, and the *caspase-8* copy number was calculated by the expression $2^{-\Delta\Delta Ct}$, where $\Delta\Delta Ct = (Ct_{casp8} - Ct_{NIK})_{sample\ DNA} - (Ct_{casp8} - Ct_{NIK})_{nondeleted\ control\ DNA}$.

Using this method, the $2^{-\Delta\Delta Ct}$ values were expected to be close to 1 in samples without *caspase8* deletions and close to 0.5 in samples with 100% *caspase-8* deletions. The percentage of *caspase-8* deletion in each sample

was deduced from the $2^{-\Delta\Delta Ct}$ values according to the following calculation: percentage of deletion = $(1 - 2^{-\Delta\Delta Ct}) \times 200$.

Results

Generation of caspase-8 conditional knockout mice

Applying the strategy used for the full knockout of *caspase-8* (13), we generated mice with conditional *caspase-8* allele (*Casp8^{F/+}*) by using a targeting construct designed to excise exons 1 and 2 that encode the two N-terminal death-effector domain motifs in the protein (Fig. 1A). ES cell clones that underwent homologous recombination with the transfected construct were transfected with a Cre-expressing construct to delete the *loxP* site-flanked selection cassette, and were then aggregated with blastocysts to generate germline-competent chimeras. Development was normal in mice homozygous for the floxed allele and in mice in which one of the *caspase-8* alleles was floxed and the other knocked out (13); *Casp8^{F/-}*, whereas *Casp8^{F/+}* mice in which the floxed allele was deleted by their mating with a Cre-deleter strain (20) (Fig. 1B) died during embryogenesis, as expected from the embryonic lethal phenotype of *caspase-8* knockout mice.

Caspase-8 plays an apoptotic role in hepatocytes in vivo

Although there is extensive evidence for caspase-8 participation in death induction in cultured cells, there is no reported direct evidence that caspase-8 serves a similar function in vivo. With the object of using Cre-mediated ablation of caspase-8 to assess the in vivo relevance of its in vitro apoptotic function we attempted to delete caspase-8 in hepatocytes, cells whose apoptotic death in response to Fas triggering has often been suggested to occur in a caspase-8-dependent manner.

Crossing the *Casp8^{F/-}* mice with a transgenic mouse line that expresses Cre under control of the liver-specific albumin promoter (*Alb-Cre*; Ref. 19) resulted in effective decrease of caspase-8 expression in the liver, but not in other organs (Fig. 2A). A real-time PCR test designed to allow quantification of *caspase-8* deletion (Fig. 1C) confirmed that deletion of the floxed allele occurred to

about the same high extent in the livers of *Casp8^{F/-}* and control *Casp8^{F/+}* mice (Fig. 2B). The *Casp8^{F/+}* Alb-Cre mice appeared normal. However, whereas injection of anti-Fas Ab (15 μ g/mouse) in the control *Casp8^{F/+}*:Alb-Cre littermates or in wild-type mice resulted in death of all mice within 6 h, the *Casp8^{F/-}*:Alb-Cre mice ($n = 20$) injected with the Ab were still alive months afterward. Histological and Western blot analysis after anti-Fas injection disclosed massive apoptosis and hemorrhage, associated with early induction of caspase-3 processing, in the livers (though not in the spleens) of control *Casp8^{F/+}*:Alb-Cre mice, but not of *Casp8^{F/-}*:Alb-Cre mice (Fig. 2, C and D).

Expression of the albumin promoter begins before birth, thus dictating deficiency of caspase-8 in the liver of the *Casp8^{F/-}*:Alb-Cre mouse almost throughout its life. To exclude the possibility that the resistance to anti-Fas observed in the *Casp8^{F/-}*:Alb-Cre mice was secondary to other changes induced in the liver owing to this prolonged caspase-8 deficiency, we crossed the *Casp8^{F/-}* mice with the *Mx1-Cre* line, which expresses Cre under the control of the α B IFN-inducible Mx1 promoter. This line responds to injection of IFN or of the IFN inducer, pI-pC, by effective induction of Cre and consequent deletion of floxed genes in various tissues, including the liver (17). As in the case of the *Casp8^{F/-}*:Alb-Cre mice, the liver cells of *Casp8^{F/-}*:*Mx1-Cre* mice in which *caspase-8* was deleted (by pI-pC injection) a few days before anti-Fas injection were resistant to the cytotoxicity of the anti-Fas Abs (Fig. 2E).

Caspase-8 function in endothelial cells plays a crucial role in embryonic development

Caspase-8 knockout embryos show evidence of circulatory failure at the time of death (13, 14). In an attempt to elucidate the mechanism underlying this failure, we specifically targeted caspase-8 in endothelial cells by crossing mice in which one of the *caspase-8* alleles had been knocked out and the other floxed (*Casp8^{F/-}*) with mice that express the Cre recombinase under control of the endothelium-specific *Tie1* promoter (Ref. 16; see Fig. 3K for demonstration of the expression pattern of this Cre transgene). Whereas

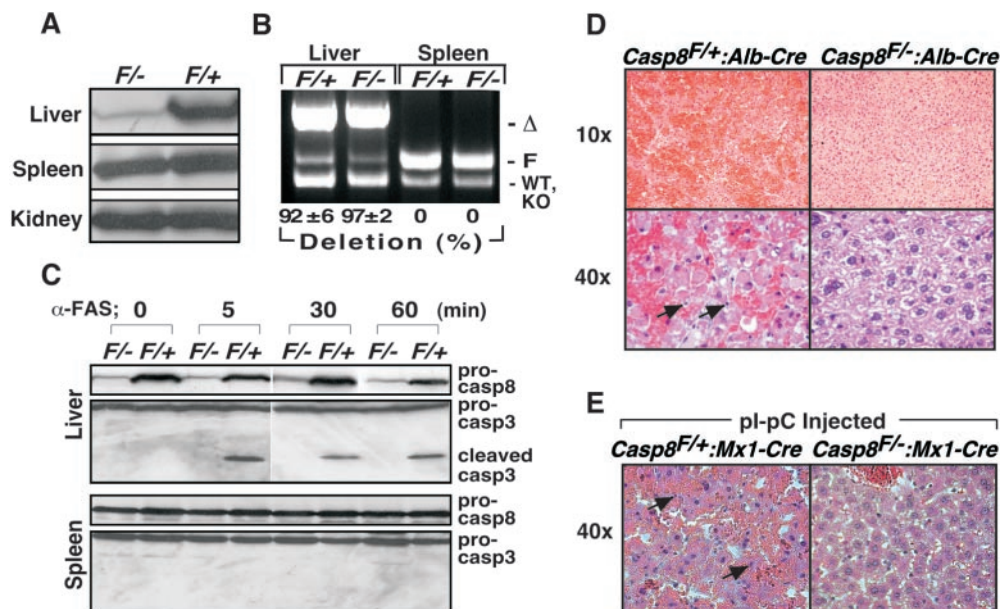


FIGURE 2. Deletion of the *caspase-8* gene in hepatocytes endows them with resistance to Fas cytotoxicity. *A–D*, Comparison of *Casp8^{F/+}*:Alb-Cre and *Casp8^{F/-}*:Alb-Cre mice. *A*, Western blot analysis of procaspase-8 expression in various tissues. *B*, Assessment of the levels of the various *caspase-8* alleles by PCR (top) and by real-time PCR (numbers at the bottom) in the livers and spleens. *C*, Evaluation of the extent of caspase-3 processing in the tissues by Western blotting at various times after their injection with anti-Fas Ab. *D*, Liver histology 6 h after injection of anti-Fas Ab. *E*, Liver histology of pI-pC-pretreated *Casp8^{F/+}*:*Mx1-Cre* and *Casp8^{F/-}*:*Mx1-Cre* mice 6 h after injection of anti-Fas Ab. Arrows in *D* and *E* point to pyknotic nuclei in apoptotic cells.

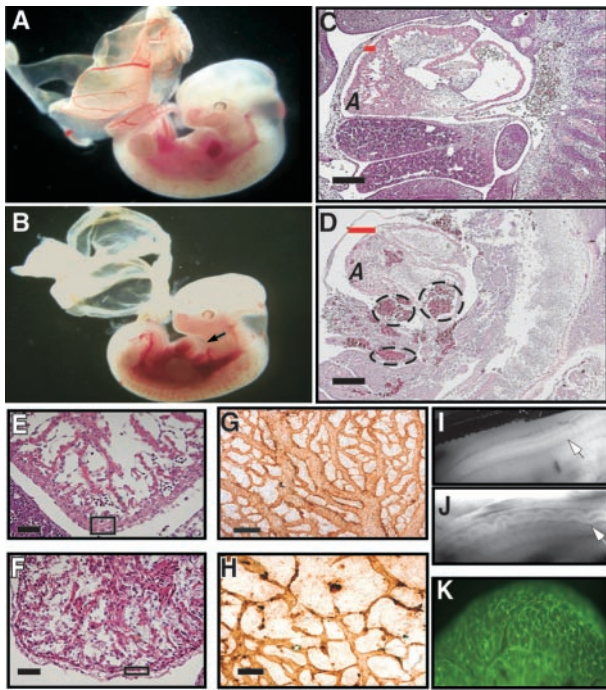


FIGURE 3. Deletion of the *caspase-8* gene in endothelial cells results in circulatory failure and cardiovascular and neural tube defects similar to those observed in full *caspase-8* knockout. *A–J*, Pathology of E11.5 *Casp8^{F/+}:Tie1-Cre* embryos at the time of their death (*B, D, F, H, J*), compared with E11.5 *Casp8^{F/+}:Tie1-Cre* embryos (*A, C, E, G, I*). *A* and *B*, Whole view, demonstrating congestion and pericardial effusion (arrow) and blood-depleted yolk sacs. *C* and *D*, Sagittal section through the whole embryo (H&E staining) demonstrating congestion (circles) as well as an expanded pericardial cavity and thinning of the chest wall (red bars) consistent with pericardial effusion, and rounding of the cardiac apex (*A*). *E* and *F*, Section through the chest demonstrating thinning of the ventricular wall (boxes) and abnormal rounding of the cardiac apex. *G* and *H*, Whole-mount anti-PECAM-1 immunostaining of the yolk sacs demonstrating extensive reduction in vascular density. *I* and *J*, View of the undulant neural tube (arrows). *K*, Green fluorescence staining in the head of an *Casp8^{F/+}:Tie1-Cre* mouse crossed with a mouse of the reporter strain (Z/EG) that expresses EGFP upon Cre-mediated excision, manifesting EGFP expression throughout the vasculature. Scale bars: *C* and *D*, 250 μ m; *E* and *F*, 50 μ m; *G* and *H*, 150 μ m.

Casp8^{F/+} mice harboring the *Tie1-Cre* transgene (*Casp8^{F/+}:Tie1-Cre*) and *Casp8^{F/-}* mice developed normally, the *Casp8^{F/-}:Tie1-Cre* mice died during embryogenesis. Death occurred at about the same time (around E12) as in *Casp8^{F/-}* mice and with the same gross pathology: severe congestion of the liver and of the large blood vessels of the chest and abdomen associated with depletion of blood from the yolk sac (Fig. 3, *A–D*). Moreover, histological analysis of *Casp8^{F/-}:Tie1-Cre* embryos that had died revealed the same abnormalities as those found in *Casp8^{F/-}* embryos (13, 14): enlargement of the pericardial space (Fig. 3, *B* and *D*) and thinning of the chest wall (Fig. 3*D*), consistent with pericardial edema; globose shape of the heart (Fig. 3, *D* and *F*) and marked attenuation, in some embryos even rupture, of the ventricular wall (Fig. 3*F*), associated with extensive necrosis of the ventricular and atrial cardiomyocytes; decreased vascular density in the yolk sac (Fig. 3*H*); and abnormally undulant neural tube (Fig. 3*J*).

To learn more about the actual mechanism of death of the *Casp8^{F/-}:Tie1-Cre* embryos, we attempted to define the sequence in which the various aberrations occur in the embryo at the time of death. Although all dying *Casp8^{F/-}:Tie1-Cre* embryos manifested severe heart muscle deformations, we could not discern such de-

formations in any of the live E10–11.5 *Casp8^{F/-}:Tie1-Cre* embryos that we examined, suggesting that they occur only a very short time before death. Most of these E10–11.5 embryos did not manifest any clear deformation of their yolk sac vasculature either. However, in the yolk sac vasculature of some of these embryos, we did discern focal sites of degeneration (Fig. 4, *A–C*). To obtain a quantitative measure of this degeneration we determined the incidence of cells positive for processed caspase-3, a marker of apoptosis, in the yolk sacs. At E10.5 it was about 4-fold higher in the yolk sacs of *Casp8^{F/-}:Tie1-Cre* embryos than in the yolk sacs of *Casp8^{F/+}:Tie1-Cre* embryos (an incidence of $0.9 \pm 0.2\%$ compared with $0.2 \pm 0.1\%$, in analysis of the yolk sacs of 10 embryos of each kind, from six litters). Notably, the increased cell death was observed even in yolk sacs that did not manifest any evident histological signs of vascular degeneration. Moreover, most of the caspase-3 positive cells in the yolk sacs were found extravascularly (arrow in Fig. 4*D*). Therefore, their occurrence implies not the death of the endothelial cells, but rather a degenerative process in the cells surrounding the yolk sac vasculature that occurs secondarily to some invisible change in the endothelial cells.

Caspase-8 is needed for the functioning of hemopoietic progenitors

Apart from circulatory failure, *Casp8^{F/-}* embryos also manifest a marked decrease in hemopoietic progenitors (13). However, in the *Casp8^{F/-}:Tie1-Cre* embryos, the levels of clonogenic progenitors observed *in vitro* were normal (data not shown). This finding suggested that the hemopoietic deficiency in the *Casp8^{F/-}* embryos reflects a function of caspase-8 in cells other than endothelial cells. To examine this possibility, we first attempted to determine whether expression of caspase-8 is required for functioning of the hemopoietic progenitors in the adult as well. The BM cells of *Casp8^{F/-}:Mx1-Cre* mice, which we examined after injecting either IFN or the IFN inducer, pI-pC, showed no change in the number of cells with staining characteristics of hemopoietic progenitors (lineage negative, *c-kit* positive; ~ 2.5 –3% of the BM cells; data

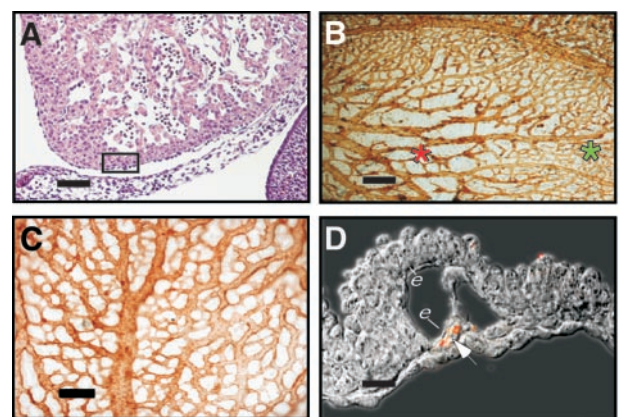


FIGURE 4. Early manifestations of the pathology in *Casp8^{F/-}:Tie1-Cre* embryos before death. *A*, Normal heart morphology and normal ventricular wall thickness (box) in an E11 embryo. *B*, Whole-mount anti-PECAM-1 immunostaining of the yolk sac of the same E11 embryo, showing degenerating vasculature (red asterisk) alongside vasculature of normal morphology (green asterisk). *C*, Whole-mount anti-PECAM-1 immunostaining of an E10.5 yolk sac with normal vasculature. *D*, Antiactive caspase-3 immunostaining (red fluorescence superimposed on the corresponding differential interference contrast image) of the same yolk sac, demonstrating extravascular location of the apoptotic cells found in increased amounts in the *Casp8^{F/-}:Tie1-Cre* yolk sacs (*e*, endothelial cells) at this stage. Scale bars: *A* and *C*, 150 μ m; *B*, 250 μ m; *D*, 10 μ m.

not shown). However, 2 days after the injection we observed a precipitous decrease in the functionality of these progenitor cells, as assessed by their ability to form myeloid or B lymphoid colonies (CFU culture (CFU-C)) in vitro (Fig. 5, A–C), form colonies in the spleens of irradiated mice (CFU-S₈ and CFU-S₁₃) (Fig. 5, D–F), and repopulate the BM and lymphoid organs of sublethally irradiated *RAG-1*^{-/-} mice with B and T lymphocytes (Fig. 6, A and B). The spleens, lymph nodes, and livers of pI-pC-injected *Casp8*^{F/+}*Mx1-Cre* mice showed a similar decrease in CFU-C, ruling out the possibility that the observed decrease of CFU-C in the BM reflected translocation of these progenitors to other organs (data not shown).

Further testing of the consequences of *caspase-8* deletion in radiation chimera of wild-type and floxed mice showed that pI-pC injection resulted in a decrease of BM CFU-C in irradiated wild-type mice that were reconstituted with *Casp8*^{F/+}*Mx1-Cre* BM cells, but not in irradiated *Casp8*^{F/-}*Mx1-Cre* mice reconstituted with wild-type BM cells (Fig. 6, C and D). Therefore, it seems that the arrest of hemopoietic progenitor function in mice deficient in caspase-8 reflects a cell-autonomous role of this enzyme.

It should be noted that although we observed no effect of IFN or pI-pC on hemopoietic progenitor function when injecting these compounds alone into *Casp8*^{F/+}*Mx1-Cre* mice (Fig. 6C, and data not shown), our data do not exclude the possibility that the arrest of hemopoietic progenitor function observed upon their injection into *Casp8*^{F/-}*Mx1-Cre* mice reflects conditioning to such an effect by caspase-8 deficiency.

Caspase-8 is needed for M-CSF-induced macrophage differentiation

The BM cells of pI-pC-injected *Casp8*^{F/+}*Mx1-Cre* mice also showed a dramatic decrease in the ability to differentiate to macrophages upon culturing with M-CSF (Fig. 7B). This finding raised the possibility that caspase-8 is required in the myeloid lineage at some later differentiation stage(s) as well. To explore this possibility, we crossed the *Casp8*^{F/-} mice with a transgenic mouse line

expressing Cre under control of the murine lysozyme M gene promoter (*LysM-Cre*), which functions in mature, lysozyme-expressing cells of the myelomonocytic lineage (18). As expected from the nondeletion of *caspase-8* at the progenitor stage in these mice, their BM cells, unlike those of the pI-pC-injected *Casp8*^{F/+}*Mx1-Cre* mice, were found to produce normal numbers of in vitro myeloid colonies (Fig. 7A). The decrease observed in the *Casp8*^{F/-}*Mx1-Cre* mice thus clearly reflects deficient functioning of progenitors before their differentiation. However, further examination of the function of the monocytic precursors in the BM of the *Casp8*^{F/-}*LysM-Cre* mice disclosed that upon differentiation they do manifest caspase-8 dependence. When incubated with M-CSF, significantly fewer F4/80⁺, CD11b⁺-adherent cells accumulated in the *Casp8*^{F/-}*LysM-Cre*-derived BM cultures (Fig. 7, C and D). Moreover, PCR and real-time PCR analyses of the prevalence of the various *caspase-8* alleles in those few *Casp8*^{F/-}*LysM-Cre* cells that did adhere revealed that these were mainly cells in which deletion of the floxed *caspase-8* allele had failed to occur (Fig. 7E). Compared with *Casp8*^{F/+}*LysM-Cre*-derived cultures, the cultures derived from *Casp8*^{F/-}*LysM-Cre* also contained larger amounts of annexin V-positive monocytic cells (Fig. 7F). Taken together, these findings suggested that M-CSF can induce differentiation only in macrophage precursors that express caspase-8, while in precursors that lack this enzyme it causes death. Such a role for caspase-8 is consistent with previous findings that caspase inhibitors inhibit macrophage differentiation and activation (28, 29).

In the presence of G-CSF, the BM cells differentiate to granulocytes, and when cultured with GM-CSF, they differentiate to dendritic cells. In contrast to the extensive decrease in M-CSF-driven macrophage differentiation, the yield of granulocytes obtained when culturing *Casp8*^{F/-}*LysM-Cre* BM cells with G-CSF was identical with that obtained with *Casp8*^{F/+}*LysM-Cre* BM cells (Fig. 7G). The yield of CFU granulocyte colonies obtained when the *Casp8*^{F/-}*LysM-Cre* BM cells were cultured in semisolid

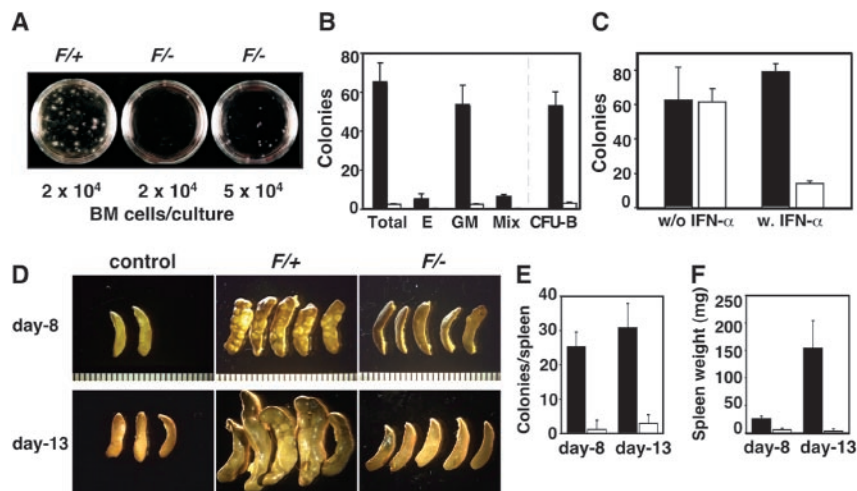


FIGURE 5. Induced ubiquitous deletion of the *caspase-8* gene compromises hemopoietic progenitor function: CFU-C and CFU-S tests. Assessments of the functionality of the hemopoietic progenitors in the BM of pI-pC-injected (A, B, D–F) and IFN-injected (C) *Casp8*^{F/+}*Mx1-Cre* and *Casp8*^{F/-}*Mx1-Cre* mice. A–C, In vitro progenitor assay. A, Gross appearance of in vitro myeloid clonogenic progenitor (CFU-C) tests, and B, yield of colonies (Total; erythroid burst-forming unit (E); CFU-granulo-macrophagic cells (GM); CFU-granulocytic-erythroid-megacaryocytic-macrophagic cells (Mix); and CFU B cells (CFU-B) in the BM of pI-pC-injected mice (mean \pm SD, $n = 8$, where n stands for the number of tests done, each with a single mouse). C, Yield of myeloid colonies in the BM of IFN-injected mice ($n = 4$). D–F, In vivo CFU-S assay. D, Appearance of spleens; E, number of colonies in the spleens ($n = 5$); and F, spleen weights in irradiated mice that were reconstituted with BM cells ($n = 5$). No colonies were detectable in the spleens of irradiated mice that were not reconstituted. Average weights of these spleens (16.7 mg on day 8 and 23.7 mg on day 13) were subtracted from the weights of the spleens of reconstituted mice. Unless otherwise indicated, solid (■) and open columns (□) in all figures correspond, respectively, to *Casp8*^{F/+} and *Casp8*^{F/-} cells.

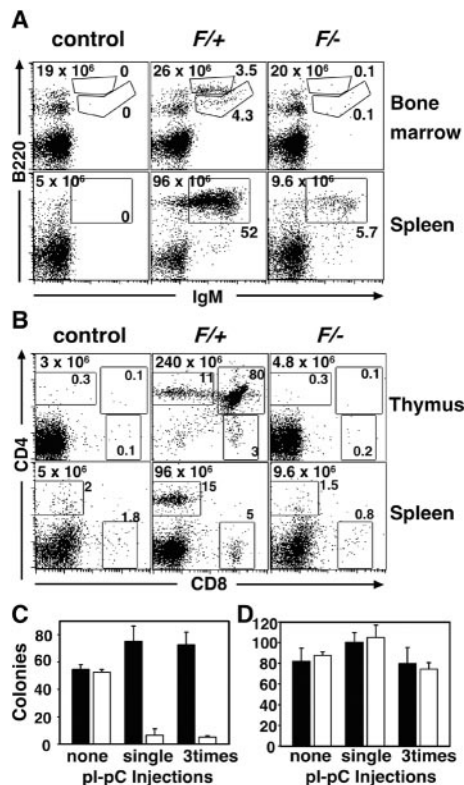


FIGURE 6. Induced ubiquitous deletion of the *caspase-8* gene compromises hemopoietic progenitor function: study of radiation chimera. *A* and *B*, Analysis of the T cell and B cell compartments in BM and lymphoid organs of irradiated *RAG-1*^{-/-} mice 7 wk after their reconstitution with the BM cells of pI-pC-injected *Casp8*^{F/+}:*Mx1-Cre* and *Casp8*^{F-/-}:*Mx1-Cre* mice (or, as a control, irradiated *RAG-1*^{-/-} mice that were not reconstituted). The cell numbers in these organs are given at the top left corners of the panels. Cell numbers in the inguinal lymph nodes were also determined, and found to be 8–14 × 10⁴ in the nonreconstituted *RAG-1*^{-/-} mice, 15–15.2 × 10⁶ in the mice reconstituted with BM cells of the *Casp8*^{F/+}:*Mx1-Cre* mice, and 6–10 × 10⁴ in the mice reconstituted with BM cells of the *Casp8*^{F-/-}:*Mx1-Cre* mice. Also shown are the percentages of living cells identified as B lymphocytes (in the BM subdivided into mature and immature) and T lymphocytes (CD4, CD8, and, in the thymus, double positive). Shown are representative data from the analysis of three transplanted mice in each of the three presented groups. Similar cell numbers were found when data from the mice were analyzed 6 mo after reconstitution (data not shown), suggesting that *caspase-8* deletion compromises the function of both committed and uncommitted hemopoietic progenitors. *C* and *D*, In vitro progenitor assay (CFU-C) of the hemopoietic progenitor levels in BM of pI-pC-injected radiation chimera. *C*, Irradiated C57BL/6 (Ly-5.1) mice reconstituted with BM cells of *Casp8*^{F/+}:*Mx1-Cre* or *Casp8*^{F-/-}:*Mx1-Cre* mice. *D*, Irradiated *Casp8*^{F/+}:*Mx1-Cre* (■) and *Casp8*^{F-/-}:*Mx1-Cre* mice (□) reconstituted with BM cells of C57BL/6 (Ly-5.1) mice (*n* = 3).

medium was also normal, as was the relative proportion of mature granulocytes within each colony (data not shown).

The yield of dendritic cells obtained upon culturing of *Casp8*^{F-/-}:*LysM-Cre* BM cells with GM-CSF was somewhat lower than in the *Casp8*^{F/+}:*LysM-Cre* BM culture (Fig. 7H). The extent of *caspase-8* deletion in the dendritic cells (which is significantly lower than in macrophages (18)) was about the same in the *Casp8*^{F-/-}:*LysM-Cre* and the *Casp8*^{F/+}:*LysM-Cre* cultures. Moreover, the extent of *caspase-8* deletion in the mature *Casp8*^{F-/-}:*LysM-Cre* dendritic cells was about the same as in the immature cells (Fig. 7, *I* and *J*) and the cells in both cultures could be fully driven to differentiation by treatment with bacterial endo-

toxin (data not shown). Thus, while apparently contributing to dendritic cell differentiation, caspase-8 seems not to serve as important a role in this process as in macrophage differentiation.

In an initial attempt to assess the implication of this finding for the in vivo occurrence of macrophages we could not discern any abnormality in the amounts or properties of the macrophages in the spleen or peritoneum of the *Casp8*^{F-/-}:*LysM-Cre* mice. However, when assessing the prevalence of the different *caspase-8* alleles in macrophages derived from peritoneal exudate cells, we found significantly less deletion of the floxed allele in the *Casp8*^{F-/-}:*LysM-Cre* peritoneal exudate cells than in the *Casp8*^{F/+}:*LysM-Cre* mice (Fig. 7K). In contrast, the extent of deletion of the floxed allele in *Casp8*^{F-/-}:*LysM-Cre* peritoneal neutrophils was about the same as that found in *Casp8*^{F/+}:*LysM-Cre* neutrophils (Fig. 7L). These findings indicated that also in vivo, ablation of *caspase-8* compromises macrophage proliferation or survival or both while having little effect on the differentiation of neutrophils.

Discussion

This study provides evidence that the functions of caspase-8 in vivo are heterogeneous with regard to both the cellular activity to which caspase-8 contributes and the physiological role of this activity. In mediating cell death induction by receptors of the TNF/NGF family, caspase-8 helps to eliminate injured and infected cells and maintain leukocyte homeostasis. Our finding that *caspase-8* deletion in hepatocytes protected these cells from Fas-mediated cytotoxicity further demonstrates, and for the first time in vivo, this immune defense-related apoptotic role. In addition, we showed in this study that caspase-8 serves some function(s) that are nonapoptotic and perhaps even antiapoptotic, and which can play a physiological role other than immune defense. Our findings indicated that in the myeloid lineage caspase-8 is needed both at an early progenitor stage and at a more differentiated monocyte precursor stage. It was also needed in B lymphocyte progenitors. According to a recent study, conditional deletion of *caspase-8* by Cre expression under control of the T cell-specific *lck* promoter compromises the expansion of activated mature T lymphocytes (30). In that model, *caspase-8* deletion had no effect on thymocyte subpopulations. Because the *lck* promoter is effectively active in thymocytes from their late double-negative stage (31), this finding suggests that, at least from that stage on, caspase-8 is not needed for thymocyte development. The present finding that deletion of caspase-8 in the BM does arrest thymocyte generation (Fig. 6B), indicates that, as in the myeloid lineage, apart from the need for caspase-8 at late differentiation stage(s), there is in the T lymphoid lineage a need for this protein also at some earlier stage(s), such as the progenitors or the early double-negative thymocytes or both. In addition, our analysis of the cause of the death of caspase-8-deficient embryos points to a developmental role of this enzyme that also appears to be nonapoptotic. This death was shown in this study to be largely, if not fully, attributable to circulatory failure resulting from caspase-8 deficiency in the endothelial cells. The earliest aberration discerned in the embryos was degeneration of the yolk sac and its vasculature. This degeneration might have occurred as a consequence of the circulatory failure. However, the fact that it preceded all other visible changes argues in favor of the opposite sequence of events. We are inclined to believe that degeneration of the yolk sac capillaries resulted from arrest of a nonapoptotic or even antiapoptotic function of caspase-8 in the endothelial cells, and that this degenerative process was the cause of the circulatory failure.

A mutation of caspase-8 that renders it enzymatically inactive and reduces its stability has been described in humans (32). Unlike

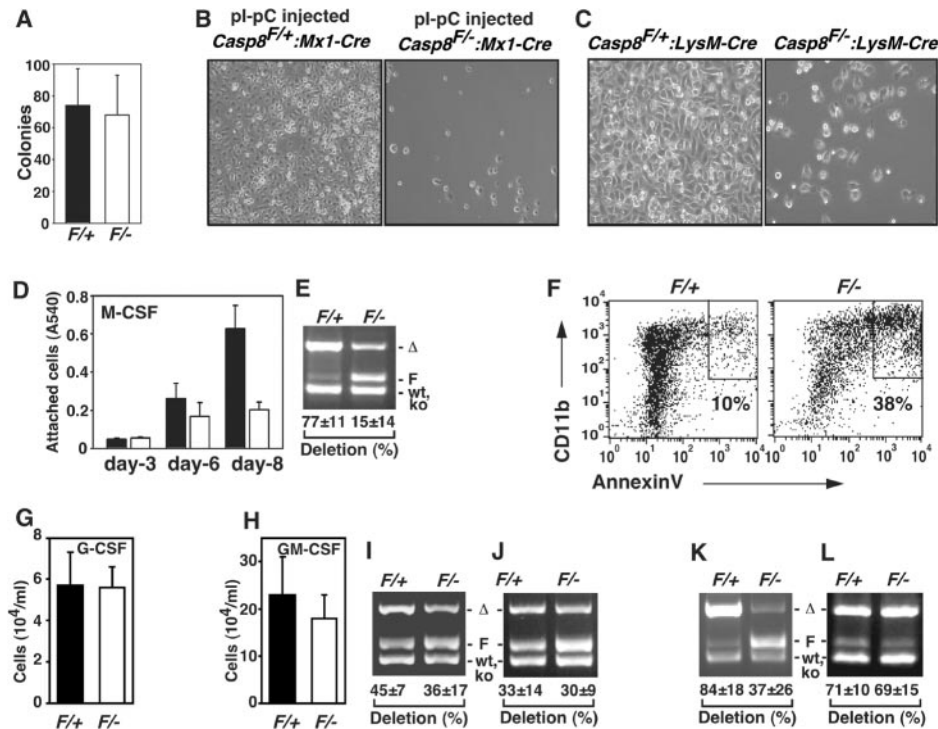


FIGURE 7. Deletion of the *caspase-8* gene in macrophage precursors compromises their differentiation. *A*, Yield of colonies in in vitro progenitor tests (CFU-C) performed with *Casp8*^{F/+}:*LysM-Cre* and *Casp8*^{F/-}:*LysM-Cre* mouse BM cells ($n = 3$). *B–J*, Features of leukocytes generated by in vitro culturing of BM cells (*B*) of pI-pC-treated *Casp8*^{F/+}:*Mx1-Cre* and *Casp8*^{F/-}:*Mx1-Cre* mice, and (*C–J*) of *Casp8*^{F/+}:*LysM-Cre* and *Casp8*^{F/-}:*LysM-Cre* mice. *C–F*, BM-derived macrophages generated by culturing with M-CSF. *B* and *C*, Appearance of adherent cells after culturing of BM cells for 7 days, and *D*, their yield after culturing for the indicated time periods ($n = 3$). *E*, Comparison of the extent of deletion of the floxed *caspase-8* allele in the adherent cells on their 7th day of culture ($n = 6$). *F*, Cell viability after 5 days in culture: FACS analysis of the nonadherent cells for expression of CD11b, a macrophage marker, and staining with annexin V, a cell death marker. *G*, Yield of granulocytes (Ly6G⁺ cells) generated by culturing of the BM cells for 7 days with mrG-CSF. *H–J*, Dendritic cells generated by culturing of the BM cells for 7 days with mrGM-CSF: *H*, yield of CD11c⁺ cells; *I*, extent of deletion of *caspase-8* in the immature CD11c⁺ MHC-II^{low}; and *J*, in the mature CD11c⁺, MHC-II^{high} dendritic cells. *K* and *L*, Extent of *caspase-8* deletion in vivo: *K*, in the peritoneal macrophages; and *L*, in the peritoneal neutrophils. Deletion was assessed by PCR (top) and real-time PCR (numbers at the bottom). WT, Wild-type *caspase-8* allele; F, floxed allele; ko, knockout allele; Δ, deleted floxed allele ($n = 4$).

the devastating impact of *caspase-8* knockout in mice, this mutation, despite interfering with leukocyte activation, seems not to affect vasculature development or compromise hemopoiesis. This difference might be attributable to the ability of caspase-10, a close homologue of caspase-8 that occurs in humans but not in mice, to compensate for caspase-8 deficiency. Alternatively, it might reflect different structural requirements for the different activities of caspase-8. Some of the activities of caspase-8 might be mediated in a way that does not depend on its proteolytic function and could therefore still be mediated in those humans with enzymatically inactive caspase-8, but not in the caspase-8-deficient mice.

As opposed to the previously described apoptotic function of caspase-8, none of its novel functions described in this study seems related to the functions of any of the known receptors of the TNF/NGF family. Nevertheless, deletion of mediator of receptor-induced toxicity-1/Fas-associated death domain protein (MORT1/FADD), the adapter protein through which caspase-8 associates with death receptors of this family, appears to have an impact quite similar to that of ablation of the function of *caspase-8*. As with *caspase-8* knockout, deletion of the *MORT1/FADD* gene in mice results in death at midgestation, associated with congestion and deformation of the heart muscle (33, 34). Like caspase-8, MORT1/FADD is also crucially involved in the fate of mature T lymphocytes, not only in their induced caspase-mediated death but also in their survival and growth (34–38). Thus, it seems that although the nonapoptotic functions of caspase-8 might be independent of the

receptors that trigger its apoptotic function, they require the same adapter protein.

The crucial involvement of the same enzyme and apparently also the same adapter protein in mediation, even in the same cell, of both apoptotic and nonapoptotic functions poses a challenge to our understanding of the mechanisms of action of these proteins. It also calls into question the completeness of our knowledge of the molecular factors determining initiation of programmed cell death.

Acknowledgments

We are grateful to Dr. Irmgard Förster for donating the *LysM-Cre* mice, Dr. Haim Cedar for his assistance in obtaining the *Mx1-Cre* mice, and Drs. Andreas Strasser and Lorraine O'Reilly for the anti-mouse caspase-8 mAb. We thank Drs. Ruth Gallily and Steffen Jung for their advice on generation and analysis of BM-derived macrophages and dendritic cells, Dr. Joseph Lotem for his advice and help with the immunohistochemistry, Dr. Ahuva Knyszynski for her assistance in generation of the conditional knockout mice, Shoshana Grossfeld for maintenance of the mice, Jadi Natan for assistance in preparation of slides for histology, and Inna Kolesnik, Raanan Margalit, Tatiana Shalevich, Dr. Yan Huang, and Dr. Shaoling Ma for technical assistance. Our thanks are also due to Dr. Lea Ersenbach, Tania Goncharov, Dr. Eli Keshet, Dr. Andrei Kovalenko, Tatyana Progozhina, Dr. Lorraine O'Reilly, and Dr. Yair Reisner for helpful advice and discussions, and to Shirley Smith for scientific editing.

References

- Jacobson, M. D., M. Weil, and M. C. Raff. 1997. Programmed cell death in animal development. *Cell* 88:347.

2. Shi, Y. 2002. Mechanisms of caspase activation and inhibition during apoptosis. *Mol. Cell* 9:459.
3. Alam, A., L. Y. Cohen, S. Aouad, and R. P. Sekaly. 1999. Early activation of caspases during T lymphocyte stimulation results in selective substrate cleavage in nonapoptotic cells. *J. Exp. Med.* 190:1879.
4. De Maria, R., A. Zeuner, A. Eramo, C. Domenichelli, D. Bonci, F. Grignani, S. M. Srinivasula, E. S. Alnemri, U. Testa, and C. Peschle. 1999. Negative regulation of erythropoiesis by caspase-mediated cleavage of GATA-1. *Nature* 401:489.
5. Kennedy, N. J., T. Kataoka, J. Tschopp, and R. C. Budd. 1999. Caspase activation is required for T cell proliferation. *J. Exp. Med.* 190:1891.
6. Faouzi, S., B. E. Burckhardt, J. C. Hanson, C. B. Campe, L. W. Schrum, R. A. Rippe, and J. J. Maher. 2001. Anti-Fas induces hepatic chemokines and promotes inflammation by an NF- κ B-independent, caspase-3-dependent pathway. *J. Biol. Chem.* 276:49077.
7. Boissonnas, A., O. Bonduelle, B. Lucas, P. Debre, B. Autran, and B. Combadiere. 2002. Differential requirement of caspases during naive T cell proliferation. *Eur. J. Immunol.* 32:3007.
8. Coletti, D., E. Yang, G. Marazzi, and D. Sasso. 2002. TNF α inhibits skeletal myogenesis through a PW1-dependent pathway by recruitment of caspase pathways. *EMBO J.* 21:631.
9. Franchi, L., I. Condo, B. Tomassini, C. Nicolo, and R. Testi. 2003. A caspase-like activity is triggered by LPS and is required for survival of human dendritic cells. *Blood* 102:2910.
10. Boldin, M. P., T. M. Goncharov, Y. V. Goltsev, and D. Wallach. 1996. Involvement of MACH, a novel MORT1/FADD-interacting protease, in Fas/APO-1- and TNF receptor-induced cell death. *Cell* 85:803.
11. Muzio, M., A. M. Chinnaiyan, F. C. Kischkel, K. O'Rourke, A. Shevchenko, J. Ni, C. Scaffidi, J. D. Bretz, M. Zhang, R. Gentz, et al. 1996. FLICE, a novel FADD-homologous ICE/CED-3-like protease, is recruited to the CD95 (Fas/APO-1) death-inducing signaling complex. *Cell* 85:817.
12. Wallach, D., E. E. Varfolomeev, N. L. Malinin, Y. V. Goltsev, A. V. Kovalenko, and M. P. Boldin. 1999. Tumor necrosis factor receptor and Fas signaling mechanisms. *Annu. Rev. Immunol.* 17:331.
13. Varfolomeev, E. E., M. Schuchmann, V. Luria, N. Chiannikulchai, J. S. Beckmann, I. L. Mett, D. Rebrikov, V. M. Brodianski, O. C. Kemper, O. Kollet, et al. 1998. Targeted disruption of the mouse Caspase 8 gene ablates cell death induction by the TNF receptors, Fas/Apo1, and DR3 and is lethal prenatally. *Immunity* 9:267.
14. Sakamaki, K., T. Inoue, M. Asano, K. Sudo, H. Kazama, J. Sakagami, S. Sakata, M. Ozaki, S. Nakamura, S. Toyokuni, et al. 2002. Ex vivo whole-embryo culture of caspase-8-deficient embryos normalize their aberrant phenotypes in the developing neural tube and heart. *Cell Death Differ.* 9:1196.
15. Nagy, A., and T. Rossant. 1993. Production of completely ES cell derived tissues. In *Gene Targeting: A Practical Approach*. A. L. Joyner, ed. Oxford Univ. Press, Oxford, p. 147.
16. Gustafsson, E., C. Brakebusch, K. Hietanen, and R. Fassler. 2001. Tie-1-directed expression of Cre recombinase in endothelial cells of embryoid bodies and transgenic mice. *J. Cell Sci.* 114:671.
17. Kuhn, R., F. Schwenk, M. Aguet, and K. Rajewsky. 1995. Inducible gene targeting in mice. *Science* 269:1427.
18. Clausen, B. E., C. Burkhardt, W. Reith, R. Renkawitz, and I. Forster. 1999. Conditional gene targeting in macrophages and granulocytes using LysMcre mice. *Transgenic Res.* 8:265.
19. Kellendonk, C., C. Opherck, K. Anlag, G. Schutz, and F. Tronche. 2000. Hepatocyte-specific expression of Cre recombinase. *Genesis* 26:151.
20. Lallemand, Y., V. Luria, R. Haffner-Krausz, and P. Lonai. 1998. Maternally expressed PGK-Cre transgene as a tool for early and uniform activation of the Cre site-specific recombinase. *Transgenic Res.* 7:105.
21. Novak, A., C. Guo, W. Yang, A. Nagy, and C. G. Lobe. 2000. Z/EG, a double reporter mouse line that expresses enhanced green fluorescent protein upon Cre-mediated excision. *Genesis* 28:147.
22. Mitsui, T., S. Watanabe, Y. Taniguchi, S. Hanada, Y. Ebihara, T. Sato, T. Heike, M. Mitsuyama, T. Nakahata, and K. Tsuji. 2003. Impaired neutrophil maturation in truncated murine G-CSF receptor-transgenic mice. *Blood* 101:2990.
23. Mosmann, T. 1983. Rapid colorimetric assay for cellular growth and survival: application to proliferation and cytotoxicity assays. *J. Immunol. Methods* 65:55.
24. Ajuenor, M. N., A. M. Das, L. Virag, R. J. Flower, C. Szabo, and M. Perretti. 1999. Role of resident peritoneal macrophages and mast cells in chemokine production and neutrophil migration in acute inflammation: evidence for an inhibitory loop involving endogenous IL-10. *J. Immunol.* 162:1685.
25. Fainaru, O., E. Woolf, J. Lotem, M. Yarmus, O. Brenner, D. Goldenberg, V. Negreanu, Y. Bernstein, D. Levanon, S. Jung, and Y. Groner. 2004. Runx3 regulates mouse TGF- β -mediated dendritic cell function and its absence results in airway inflammation. *EMBO J.* 23:969.
26. Laird, P. W., A. Zijderveld, K. Linders, M. A. Rudnicki, R. Jaenisch, and A. Berns. 1991. Simplified mammalian DNA isolation procedure. *Nucleic Acids Res.* 19:4293.
27. Livak, K. J., and T. D. Schmittgen. 2001. Analysis of relative gene expression data using real-time quantitative PCR and the $2^{-\Delta\Delta CT}$ method. *Methods* 25:402.
28. Kim, S. O., K. Ono, and J. Han. 2001. Apoptosis by pan-caspase inhibitors in lipopolysaccharide-activated macrophages. *Am. J. Physiol.* 281:L1095.
29. Sordet, O., C. Rebe, S. Plenchette, Y. Zermati, O. Hermine, W. Vainchenker, C. Garrido, E. Solary, and L. Dubrez-Daloz. 2002. Specific involvement of caspases in the differentiation of monocytes into macrophages. *Blood* 100:4446.
30. Salmena, L., B. Lemmers, A. Hakem, E. Matysiak-Zablocki, K. Murakami, P. Y. Au, D. M. Berry, L. Tamblyn, A. Shehabeldin, E. Migon, et al. 2003. Essential role for caspase 8 in T-cell homeostasis and T-cell-mediated immunity. *Genes Dev.* 17:883.
31. Buckland, J., D. J. Pennington, L. Bruno, and M. J. Owen. 2000. Co-ordination of the expression of the protein tyrosine kinase p56^{lck} with the pre-T cell receptor during thymocyte development. *Eur. J. Immunol.* 30:8.
32. Chun, H. J., L. Zheng, M. Ahmad, J. Wang, C. K. Speirs, R. M. Siegel, J. K. Dale, J. Puck, J. Davis, C. G. Hall, et al. 2002. Pleiotropic defects in lymphocyte activation caused by caspase-8 mutations lead to human immunodeficiency. *Nature* 419:395.
33. Yeh, W. C., J. L. Pompa, M. E. McCurrach, H. B. Shu, A. J. Elia, A. Shahinian, M. Ng, A. Wakeham, W. Khoo, K. Mitchell, et al. 1998. FADD: essential for embryo development and signaling from some, but not all, inducers of apoptosis. *Science* 279:1954.
34. Zhang, J., D. Cado, A. Chen, N. H. Kabra, and A. Winoto. 1998. Fas-mediated apoptosis and activation-induced T-cell proliferation are defective in mice lacking FADD/Mort1. *Nature* 392:296.
35. Walsh, C. M., B. G. Wen, A. M. Chinnaiyan, K. O'Rourke, V. M. Dixit, and S. M. Hedrick. 1998. A role for FADD in T cell activation and development. *Immunity* 8:439.
36. Newton, K., A. W. Harris, M. L. Bath, K. G. Smith, and A. Strasser. 1998. A dominant interfering mutant of FADD/MORT1 enhances deletion of autoreactive thymocytes and inhibits proliferation of mature T lymphocytes. *EMBO J.* 17:706.
37. Zornig, M., A. O. Hueber, and G. Evan. 1998. p53-dependent impairment of T-cell proliferation in FADD dominant-negative transgenic mice. *Curr. Biol.* 8:467.
38. Kabra, N. H., C. Kang, L. C. Hsing, J. Zhang, and A. Winoto. 2001. T cell-specific FADD-deficient mice: FADD is required for early T cell development. *Proc. Natl. Acad. Sci. USA* 98:6307.